



OPEN

Selective detection of endogenous H₂S in living cells and the mouse hippocampus using a ratiometric fluorescent probe

SUBJECT AREAS:
CHEMICAL TOOLS
BIOMARKER RESEARCHLing Zhang^{1,2*}, Wen-qi Meng^{2*}, Liang Lu¹, Yun-Sheng Xue², Cheng Li², Fang Zou², Yi Liu² & Jing Zhao^{1,3}Received
22 April 2014Accepted
10 July 2014Published
29 July 2014Correspondence and
requests for materials
should be addressed to
J.Z. (jingzhao@nju.
edu.cn) or Y.L.
(cbpe201087@gmail.
com)* These authors
contributed equally to
this work.

¹State Key Laboratory of Pharmaceutical Biotechnology, School of Life Sciences, Institute of Chemistry and BioMedical Sciences, Nanjing University, Nanjing, 210093, China, ²School of Pharmacy, Xuzhou Medical College, Xuzhou, 221002, China, ³Guangdong Key Lab of Nano-Micro Material Research, School of Chemical Biology and Biotechnology, Shenzhen Graduate School of Peking University, Shenzhen, 518055, China.

As one of three gasotransmitters, the fundamental signalling roles of hydrogen sulphide are receiving increasing attention. New tools for the accurate detection of hydrogen sulphide in cells and tissues are in demand to probe its biological functions. We report the *p*-nitrobenzyl-based ratiometric fluorescent probe RHP-2, which features a low detection limit, high selectivity and good photostability. The emission intensity ratios had a good linear relationship with the sulphide concentrations in PBS buffer and bovine serum. Our probe was applied to the ratiometric determination and imaging of endogenous H₂S in living cells. Furthermore, RHP-2 was used as an effective tool to measure endogenous H₂S in the mouse hippocampus. We observed a significant reduction in sulphide concentrations and downregulated expression of cystathionine β-synthetase (CBS) mRNA and CBS protein in the mouse hippocampus in a chronic unpredictable mild stress (CUMS)-induced depression model. These data suggested that decreased concentrations of endogenous H₂S may be involved in the pathogenesis of chronic stress depression.

Hydrogen sulphide (H₂S) has been identified as an endogenous gaseous signalling molecule as well as a cytoprotectant^{1,2}. Endogenous H₂S is primarily produced in the mitochondria or cytosol from a cysteine substrate, or its derivatives, with catalysis by enzymes such as cystathionine β-synthetase (CBS), cystathionine γ-lyase (CSE) and cysteine aminotransferase (CAT)/3-mercaptopyruvate sulphurtransferase (3-MST)³. Physiological concentrations of H₂S are associated with the regulation of diverse biological functions, including vasodilation, apoptosis, neurotransmission, ischemia/reperfusion-induced injury, insulin secretion and inflammation^{4–9}. In addition, H₂S protects the cardiovascular and central nervous systems from oxidative stress¹⁰. The misregulation of endogenous H₂S is present in many diseases^{11–14}, such as Down syndrome, Alzheimer's disease (AD), Parkinson's disease (PD) and febrile seizures. However, the detailed molecular pathways of H₂S are not fully understood, partly due to the lack of non-invasive and real-time detection techniques for H₂S.

Current approaches to H₂S detection include the methylene blue method, the monobromobimane method (MBB), gas chromatography (GC) and the sulphide ion selective electrodes (ISE) method^{15–20}. However, these methods often require the extraction of sulphide from tissues or cells. For the dynamic monitoring of H₂S in biological specimens, small-molecule fluorescent probes have recently emerged as an effective tool for the detection and imaging of H₂S. Detection mechanisms may involve trapping H₂S via nucleophilic addition, copper sulphide precipitation, H₂S-mediated reduction, or the thiolysis of dinitrophenyl ether by H₂S^{21–31}. Compared with “turn-on” fluorescent probes, ratiometric fluorescent probes are more accurate for detecting H₂S, independently of variables in quantitative analysis such as excitation intensity variations, environmental factors, light scattering and probe concentrations³².

As a result of the reduction of nitro groups to amino groups under hypoxic conditions, several research groups have reported nitro-based fluorescent probes for imaging hypoxic status via the detection of nitroreductase^{33–37}. We were especially interested in the *p*-nitrobenzyl-based hypoxia probe (referred to as RHP) reported by Qian *et al.* that is synthetically accessible and has robust efficacy *in vitro*³⁸. Additionally, there are several reports on the development of H₂S-specific probes based on the nitro-reduction mechanism by H₂S^{39–42}. Accordingly, we hypothesised that the *p*-nitrobenzyl moiety is applicable to H₂S identification under normoxic conditions. Herein, we describe the ratiometric fluorescent probe RHP-2 for the selective detection of H₂S, featuring the

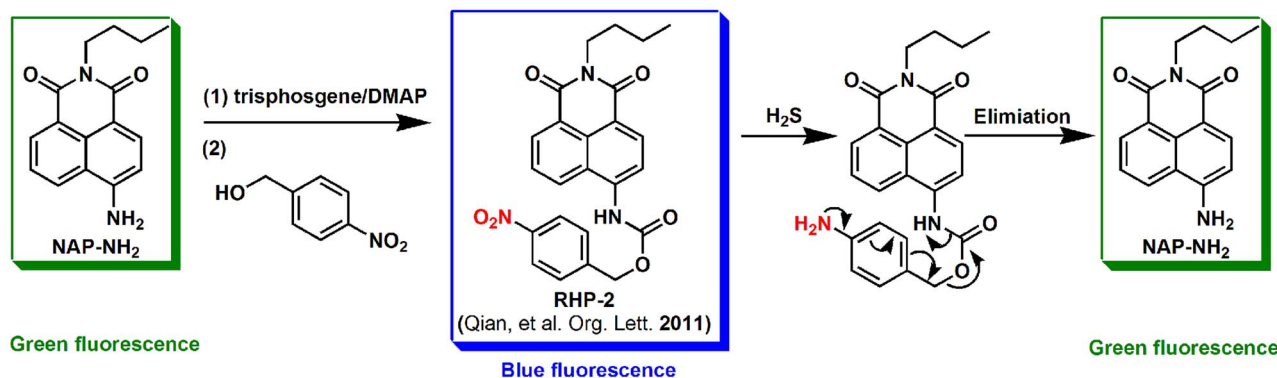


Figure 1 | The synthesis of RHP-2 and the detection mechanism of H₂S using RHP-2 (RHP-2 was first designed for hypoxia by Qian *et al.* in 2011).

same scaffold as the RHP probe by Qian (Fig. 1). Using the RHP-2 probe, we detected and imaged the endogenous H₂S in MCF-7 cells and measured endogenous H₂S in the mouse hippocampus.

Results

Synthesis and sensing mechanism. We employed 1,8-naphthalimide as an intramolecular charge transfer (ICT) fluorophore owing to its desirable spectroscopic properties and feasibility in structural modification. The nitro group served as the H₂S reaction site. Probe RHP-2 was constructed by connecting a *p*-nitrobenzyl group to 1,8-naphthalimide via a carbamate-linkage. The electron-withdrawing carbamate group weakened the ICT effect, resulting in blue shifts in emission. The ratiometric detection of sulphide, as anticipated, involved the reaction of RHP-2 with sulphide, in which *p*-nitrobenzyl was reduced to *p*-aminobenzyl by H₂S under the normoxic conditions, the carbamate group was cleaved, and the green fluorescence of the compound NAP-NH₂ was restored (Fig. 1). RHP-2 was readily synthesised as described in Figure 1, and was characterised by NMR spectroscopy and mass spectrometry (refer to the supplementary information).

To assess the reaction mechanism of RHP-2 with sulphide, RHP-2 was incubated with Na₂S (a common hydrogen sulphide donor), resulting in a green fluorescent product that was identified as NAP-NH₂ based on fluorescence emission and ¹H and ¹³C NMR spectra (refer to the supplementary information). The reaction between RHP-2 and sulphide proceeded as depicted in Figure 1.

Fluorescent properties of RHP-2. The sensitivity of RHP-2 (5 μM) to sulphide was determined at 37°C in 20 mM PBS buffer (pH 7.4). In the absence of Na₂S, RHP-2 displayed a fluorescence emission maximum at 467 nm ($\Phi = 0.12$). Upon treatment of RHP-2 with a cascade of Na₂S (0–100 μM), the fluorescence intensity gradually decreased at 467 nm with the concomitant generation of a new emission peak at 532 nm ($\Phi = 0.13$) (Fig. 2A). The fluorescence emission colour of the solution changed from blue to green (Fig. 2A insert), indicating that RHP-2 is a ratiometric fluorescent probe for sulphide. The ICT mechanism of RHP-2 was further demonstrated by the density functional theory (DFT) (refer to the supplementary information).

Figure 2B depicts elevated emission intensity ratios with increasing concentrations of Na₂S until a plateau is reached at 300 μM Na₂S, suggesting that complete reaction between RHP-2 and Na₂S occurs at the concentration ratio of 1 : 60. Enhancements of 27-fold and 26-fold in emission intensity ratios were observed, from 0.34 and 0.31 for PBS buffer and serum, respectively, in the absence of Na₂S to 9.0 and 8.2 for PBS buffer and serum, respectively, in the presence of 10 equiv. Na₂S (Fig. 2B). Furthermore, the emission intensity ratios showed an excellent linear relationship with Na₂S concentrations from 0–100 μM. The detection limit for sulphide was 270 nM and 280 nM in PBS buffer and foetal bovine serum, respectively

(Supplementary Fig. S2). These results indicate that RHP-2 is sensitive to sulphide and is suitable for the quantitative analysis of endogenous H₂S in complex biological systems.

The reaction of RHP-2 with sulphide was completed in approximately 40 min (Supplementary Fig. S3). Under pseudo-first-order conditions, the rate constant for sulphide was $1.0 \times 10^{-3} \text{ s}^{-1}$ (Supplementary Fig. S4). Furthermore, the plot of k_{obs} vs. [Na₂S] formed a straight line passing through the origin, suggesting that the reaction was overall second order with $k_2 = 5.0 \text{ M}^{-1} \text{ s}^{-1}$ (Supplementary Fig. S4). As shown in Figure S5, the maximum peaks of emission intensity ratios were between pH 6.2 and 9.0, and the minimum emission intensity ratios were between pH 4.2 and 5.0. These results could be due to the inhibition of carbamate cleavage from RHP-2 under acidic conditions. The ratios of the free probe exhibited almost no changes between pH 6.2 and 9.0. Thus, RHP-2 can serve as a fluorescent ratiometric probe for sulphide between pH 6.2 and 9.0.

Subsequently, the determination of the photostability of RHP-2 was conducted, in which an RHP-2 solution was exposed to visible light and UV light for 60 min, and no changes in the emission intensities of RHP-2 were observed (Supplementary Fig. S6).

Selectivity of RHP-2. The selectivity of RHP-2 for sulphide was examined. As shown in Figure 3A, RHP-2 was selective for sulphide in the absence of interference with biothiols, such as glutathione (GSH), cysteine (Cys) and homocysteine (Hcy). The remaining non-thiol amino acids (Ala, Glu, Trp, Met, Tyr, Leu, Val, Ser, Pro, Arg, Gly, Phe, His, Gln, Asn, Ile and Thr), inorganic salts (KCl, CaCl₂, NaCl, MgCl₂, FeCl₃, ZnSO₄ and NaH₂PO₄), reactive oxygen species (H₂O₂, $\cdot\text{OCl}^-$, O₂⁻, $\cdot\text{OH}$ and ^tBuOOH), reactive nitrogen species (NO₂⁻ and NO), reducing agents (NADH and glucose), sulphur-containing inorganic ions (S₂O₃²⁻, S₂O₅²⁻, SO₄²⁻, S₂O₄²⁻, SO₃²⁻ and SCN⁻) and S-nitroso glutathione (SNG) showed negligible responses (Figs. 3B, 3C, 3D and S8). Additionally, competitive experiments revealed minimal interference with sulphide detection in the coexistence of various species and Na₂S. The emission intensity ratios decreased only in the presence of H₂O₂ and ZnSO₄ (Fig. 3C), which may be attributed to the oxidation of H₂S by H₂O₂ and sulphide precipitation of H₂S by ZnSO₄. Accordingly, RHP-2 is applicable to the selective determination of sulphide with minimal interference with these biological species.

Detection of H₂S in living cells. We tested the potential utility of RHP-2 for ratiometric fluorescence imaging of H₂S in living MCF-7 cells. Prior to cell imaging, MTT assays were conducted to evaluate the cytotoxicity of RHP-2 and NAP-NH₂. RHP-2 and NAP-NH₂ showed IC₅₀ values of 101.2 ± 1.3 and 82.6 ± 1.1 μM, respectively (Supplementary Figs. S9 and S10), indicating the low toxicity of RHP-2 and NAP-NH₂ in cultured MCF-7 cells. The cell viability of RHP-2 and NAP-NH₂ at 0, 6, 12, 18 and 24 hours further

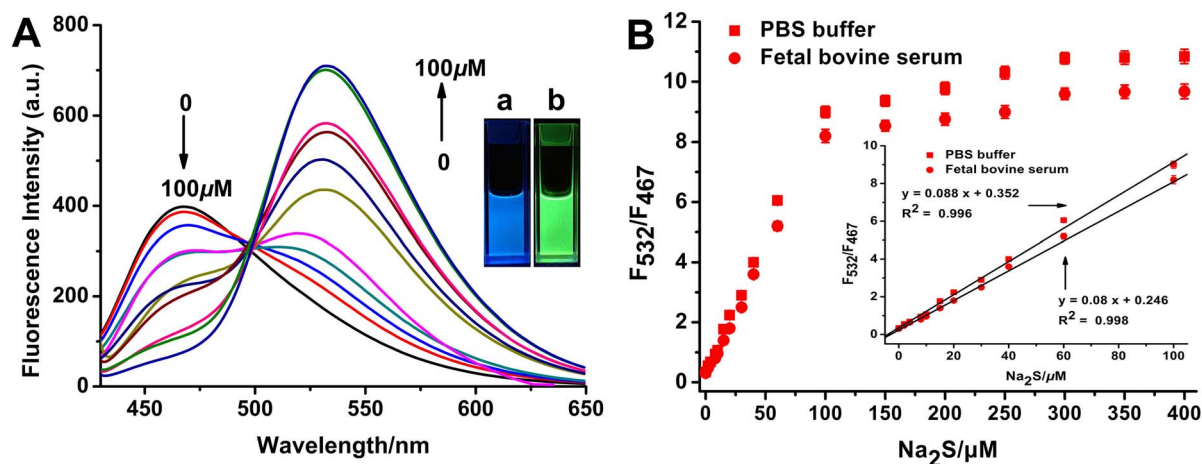


Figure 2 | Ratiometric fluorescence response of RHP-2 to sulphide. (A) Fluorescence spectra of RHP-2 (5 μM) with Na_2S (0, 2, 4, 8, 10, 15, 20, 30, 40, 60 and 100 μM) in PBS buffer (20 mM, pH = 7.4, 5% CH_3CN) at 37°C for 40 min. Insert: Photograph showing the visual fluorescence of RHP-2 without (a) or with (b) Na_2S under a 365-nm UV lamp. (B) Emission intensity ratios of RHP-2 (5 μM) after 40 min of incubation with different concentrations of Na_2S (0 to 400 μM) in PBS buffer (20 mM, pH = 7.4, 5% CH_3CN) and foetal bovine serum (5% CH_3CN). Insert: The linear relationship between the emission intensity ratios (F_{532}/F_{467}) and the concentrations of Na_2S (0 to 100 μM) in PBS buffer and foetal bovine serum. Data are presented as the mean \pm SD ($n = 3$).

demonstrated that RHP-2 and NAP-NH₂ did not affect cell viability at 5 μM (Supplementary Figs. S9 and S10).

MCF-7 cells incubated with the free probe for 30 min showed high fluorescence intensity in the blue channel, while dim fluorescence was observed in the green channel (Fig. 4, panels 1A, 1B, 1C, and 1D). In contrast, upon addition of Na_2S (300 μM) to the above cells and incubation for 20 min, a marked elevation of green fluorescence intensity was detected (Fig. 4, panels 2A, 2B, 2C, and 2D), which was consistent with the H₂S-induced ratiometric fluorescent response. After incubation with Na_2S for 40 min, the cells exhibited bright fluorescence in the green channel and faint fluorescence in the blue channel (Fig. 4, panels 3A, 3B, and 3C). Additionally, increases in the emission intensity ratios ($R = 0.63$ in column A, $R = 1.62$ in column B, $R = 3.0$ in column C) are observed in Fig. 4 (panel 4C), indicating that RHP-2 reacted with sulphide in cells to produce the green fluorescent NAP-NH₂. The treatment of probe-loaded cells at a lower sulphide concentration (Na_2S , 50 μM) for 40 min also led to a marked elevation in the intensity of green fluorescence (Supplementary Fig. S12, panel 6B) and emission intensity ratio (Supplementary Fig. S13, $R = 1.14$ in column B), implying that RHP-2 can be used to detect different sulphide concentrations in living cells. RHP-2-labeled cells were monitored and scanned at three designated sites for 60 min (Fig. 4, panel 4A), revealing stable fluorescence intensities (Fig. 4, panel 4B) and good photostability of RHP-2.

We then explored the kinetics of the reaction between RHP-2 and sulphide in living cells. Fig. 4 (panel 4D) depicts a sulphide-induced increase in emission intensity ratios in regions e and f in Fig. 4 (panel 3C), with a plateau appearing at approximately 40 min. To verify that the fluorescence change in the cells arises from H₂S, cells were pretreated with ZnCl_2 (which eliminates H₂S) (Supplementary Fig. S12, panels 7A, 7B, 7C and 7D) and subsequently incubated with RHP-2. There was no significant difference between the two emission intensity ratios in the absence (Fig. 4, panel 4C, $R = 0.63$ in column A) and presence of ZnCl_2 (Supplementary Fig. S13, $R = 0.62$ in column C), suggesting that the introduction of ZnCl_2 into the cells minimally affected the fluorescence response of RHP-2. With the addition of Na_2S (300 μM) to the ZnCl_2 -pretreated cells (Supplementary Fig. S12, panels 8A, 8B, 8C and 8D), no green fluorescence intensity and emission intensity ratio (Supplementary Fig. S13, $R = 0.63$ in column D) increases were observed. The results

indicated that the variation in the emission intensity ratio of RHP-2 resulted from the reaction with H₂S.

Subsequently, we tested the use of RHP-2 to visualise endogenous H₂S. CSE is an important H₂S-producing enzyme that can be up-regulated by NO, resulting in an increase in H₂S concentration⁴³. Accordingly, we employed SNP (sodium nitroprusside, a NO donor) to stimulate the generation of endogenous H₂S. Upon the addition of RHP-2 (5 μM) to SNP (200 μM)-loaded cells (Fig. 5, panels 1A, 1B, 1C, and 1D), a notable increase in the emission intensity ratio was observed (Fig. 4, panel 4C, $R = 1.10$ in column D), indicating the generation of endogenous H₂S within the cells. As exhibited in Figure 5 (panels 2A, 2B, 2C, and 2D), the fluorescence intensity in the green channel, along with the emission intensity ratio (Fig. 4, panel 4C, $R = 1.65$ in column E), was substantially elevated with the increased concentration of SNP (400 μM). Next, we performed a parallel experiment by pretreating the cells with DL-propargylglycine (PPG, an inhibitor of CSE) (Fig. 5, panels 3A, 3C; Supplementary Fig. S14). Upon pretreating the cells with PPG, the variation of the emission intensity ratio was negligible (Fig. 4, panel 4C, $R = 0.65$ in column F). With the addition of SNP to the PPG-pretreated MCF-7 cells, neither an increase in green fluorescence nor a decrease in blue fluorescence was observed, and a low emission intensity ratio was retained (Fig. 4, panel 4C, $R = 0.66$ in column G; Fig. 5, panels 4A and 4C; Supplementary Fig. S14). The results showed that enzyme inactivation can suppress the production of endogenous H₂S. These results established that RHP-2 is biocompatible and capable of ratiometrically imaging endogenous H₂S in living cells.

Determination of endogenous sulphide in the mouse hippocampus. Hydrogen sulphide plays important roles in regulating CNS function and is known to regulate LTP by activating NMDA receptors in neurons, eliciting Ca^{2+} waves, increasing Ca^{2+} levels and regulating intracellular pH in neurons and glial cells⁴. Moreover, H₂S has been reported to exert neuroprotective effects via various mechanisms⁴, including antioxidative, anti-inflammatory and anti-apoptotic effects. In addition to its physiological roles as a neuromodulator and as a neuroprotectant, H₂S is also involved in the pathophysiology of the CNS. Currently, controversy remains as to the actual concentration of H₂S in brain tissues, ranging from undetectable to over 100 μM , thus indicating that new methods for accurate determination of H₂S are in high demand^{44–47}.

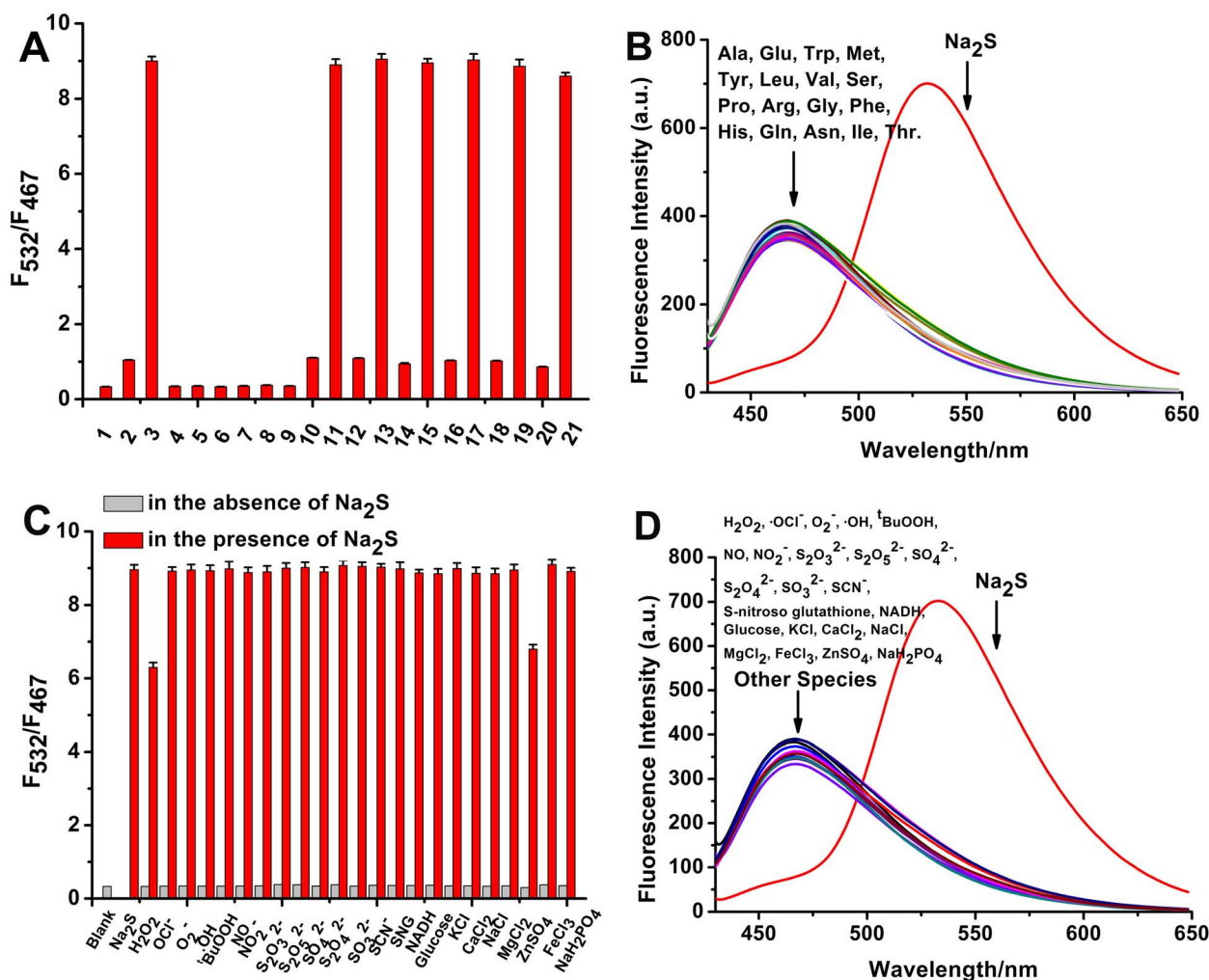


Figure 3 | The selectivity of RHP-2 for sulphide. (A) Fluorescence responses of RHP-2 (5 μM) towards Na_2S (100 μM) and various biothiols after 40 min of incubation. 1. Na_2S (0 μM); 2. Na_2S (10 μM); 3. Na_2S (100 μM); 4. Cys (100 μM); 5. Cys (1 mM); 6. Hcy (100 μM); 7. Hcy (1 mM); 8. GSH (1 mM); 9. GSH (10 mM); 10. Na_2S (10 μM) + Cys (100 μM); 11. Na_2S (100 μM) + Cys (100 μM); 12. Na_2S (10 μM) + Cys (1 mM); 13. Na_2S (100 μM) + Cys (1 mM); 14. Na_2S (10 μM) + Hcy (100 μM); 15. Na_2S (100 μM) + Hcy (100 μM); 16. Na_2S (10 μM) + Hcy (1 mM); 17. Na_2S (100 μM) + Hcy (1 mM); 18. Na_2S (10 μM) + GSH (1 mM); 19. Na_2S (100 μM) + GSH (1 mM); 20. Na_2S (10 μM) + GSH (10 mM); and 21. Na_2S (100 μM) + GSH (10 mM). (B) Fluorescence spectra of RHP-2 (5 μM) with Na_2S (100 μM) and various amino acids (1 mM) after 40 min of incubation. (C, D) Fluorescence responses of RHP-2 (5 μM) towards Na_2S (100 μM), ROS (1 mM), RNS (1 mM), sulphur-containing inorganic ions (1 mM), reducing agents (1 mM), inorganic salts (1 mM) and S-nitroso-glutathione (SNG, 1 mM) after 40 min of incubation. Data are presented as the mean \pm SD ($n = 3$).

Prompted by the promising results of selectivity, sensitivity and linearity measurements, we utilised RHP-2 to determine sulphide concentrations in the mouse hippocampus. Accordingly, the measurement of sulphide concentrations in the mouse hippocampus was conducted based on our previous method⁴⁸. In brief, fresh hippocampus homogenate was centrifuged, and the supernatant was obtained. PBS buffer, RHP-2 and Na_2S (as the internal criterion) were incubated with the supernatant for 40 min at 37 $^\circ\text{C}$. As shown in Table 1 (Supplementary Fig. S15), the median sulphide concentration in the mouse hippocampus was $1.67 \pm 0.08 \mu\text{mol g}^{-1}$ protein. The validity of our present method was verified using our previous fluorescence probe SFP-2⁴⁹ (Table 1 and Fig. S16). The values obtained by RHP-2 were similar to those obtained by SFP-2, suggesting that RHP-2 is suitable for the determination of endogenous sulphide in biological tissues.

Determination of endogenous sulphide in the hippocampus in mouse models of CUMS-induced depression. Depression, a widespread incapacitating psychiatric condition, imposes a substantial

health threat to society. Unlike studies addressing AD and PD, little is known about the role of endogenous H_2S in the pathogenesis of depression. H_2S has been reported to exert specific antidepressant-like and anxiolytic-like effects in behavioural models of depression and anxiety in mice⁵⁰. Thus, it would be interesting to investigate the pathological correlations between endogenous H_2S concentrations and depression. We established a chronic unpredictable mild stress (CUMS)-induced depression-like model in mice. Adult male Kunming mice weighing 20–25 g were randomised into three groups: control group (without treatment), model group (5-week CUMS induction) and NaHS group (5-week CUMS induction and intraperitoneal injection of NaHS at the dose of 5 mg/kg⁵⁰). At week 5, mice underwent the sucrose preference, forced swimming and tail suspension tests to evaluate depressive behaviour, followed by the determination of sulphide concentrations and CBS mRNA levels and CBS protein expression in the mouse hippocampus.

There was no significant difference in sucrose consumption among the three groups prior to CUMS induction (Supplementary

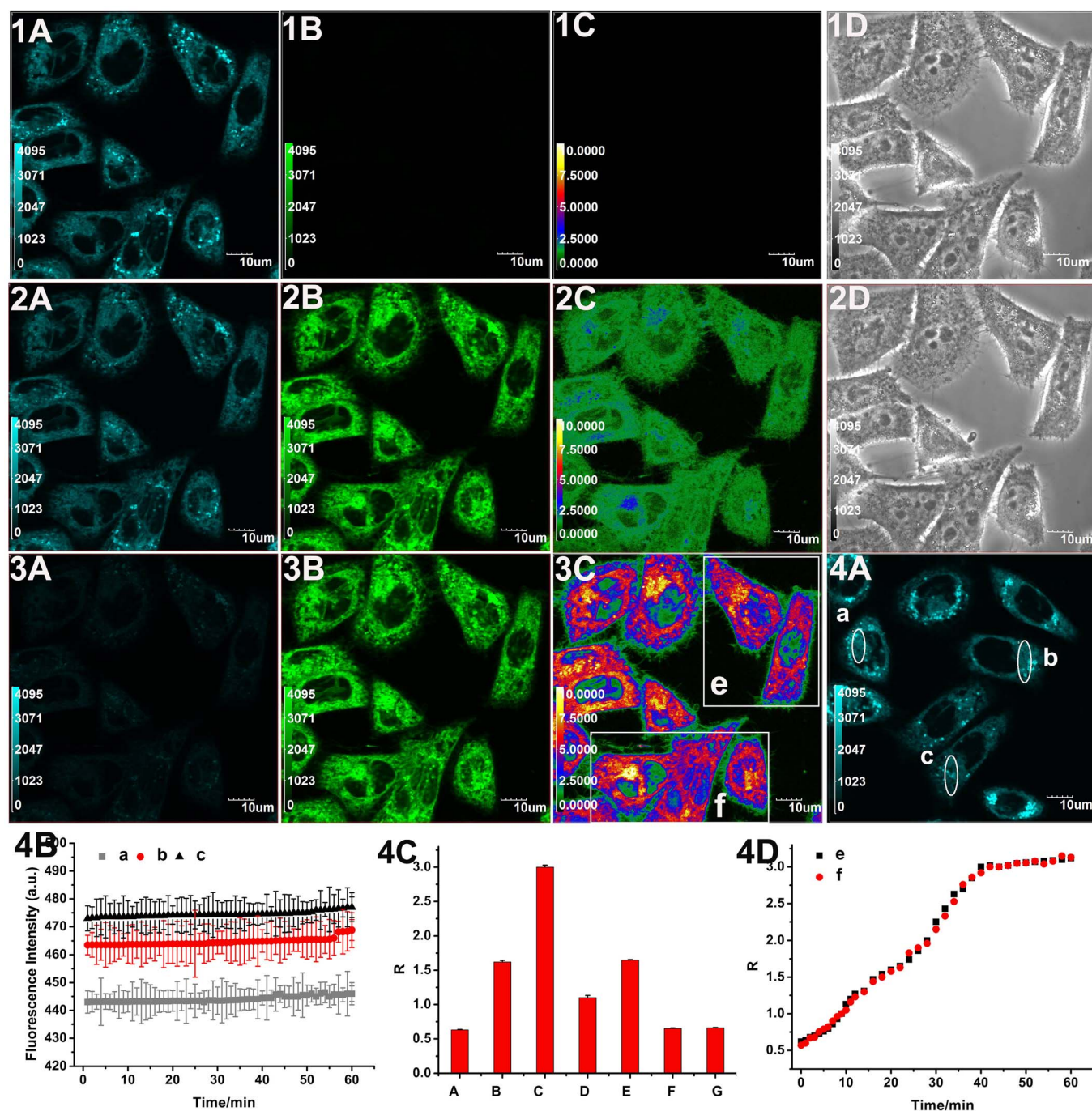


Figure 4 | Confocal fluorescence imaging of exogenous sulphide in living MCF-7 cells using RHP-2. Cells were incubated with RHP-2 (5 μ M) for 30 min (1A, 1B, 1C and 1D). Cells in panels 1A, 1B, 1C and 1D were then treated with Na_2S (300 μ M) for 20 min (2A, 2B, 2C, and 2D) and 40 min (3A, 3B, 3C and 3D). Blue channel images were obtained from 445 nm to 495 nm (1A, 2A and 3A). Green channel images were obtained from 520 nm to 580 nm (1B, 2B and 3B). Ratiometric images ($F_{520-580 \text{ nm}}/F_{445-495 \text{ nm}}$) were generated by Olympus software (1C, 2C and 3C) and the corresponding bright images were shown in 1D and 2D. Cells were incubated with RHP-2 (5 μ M) alone for 60 min (4A). The average fluorescence intensities were recorded at 60-s intervals in three designated sites (a, b and c) shown in panel 4A (4B) (mean \pm SD, $n = 3$). The average fluorescence emission intensity ratios ($R = F_{520-580 \text{ nm}}/F_{445-495 \text{ nm}}$) according to the corresponding ratiometric images of cells (4C) (mean \pm SD, $n = 3$). Temporal profiles of average emission intensity ratios (R) at two designated sites (e and f) in panel 3C (4D) (mean \pm SD, $n = 3$). Scale bars = 10 μ m.

Fig. S17, $p > 0.05$). At the end of the 5-week stress, sucrose consumption in the CUMS mice was remarkable lower than that in the control group (Supplementary Fig. S17, $p < 0.001$). NaHS treatment significantly increased sucrose consumption compared to the CUMS group (Supplementary Fig. S17, $p < 0.001$). CUMS-induced depressive mice showed a significant increase in immobility duration in the tail suspension test (Supplementary Fig. S18, $p < 0.001$) and the

forced swimming test compared to the control group (Supplementary Fig. S19, $p < 0.001$), demonstrating that CUMS successfully induced a depression-like state in mice. As shown in Figure 6 (Supplementary Table S1), sulphide concentrations ($p < 0.001$), expression of CBS protein ($p < 0.001$) and CBS mRNA ($p < 0.001$) in the hippocampus of the model group were significantly lower than those in the control group. However, there was significant

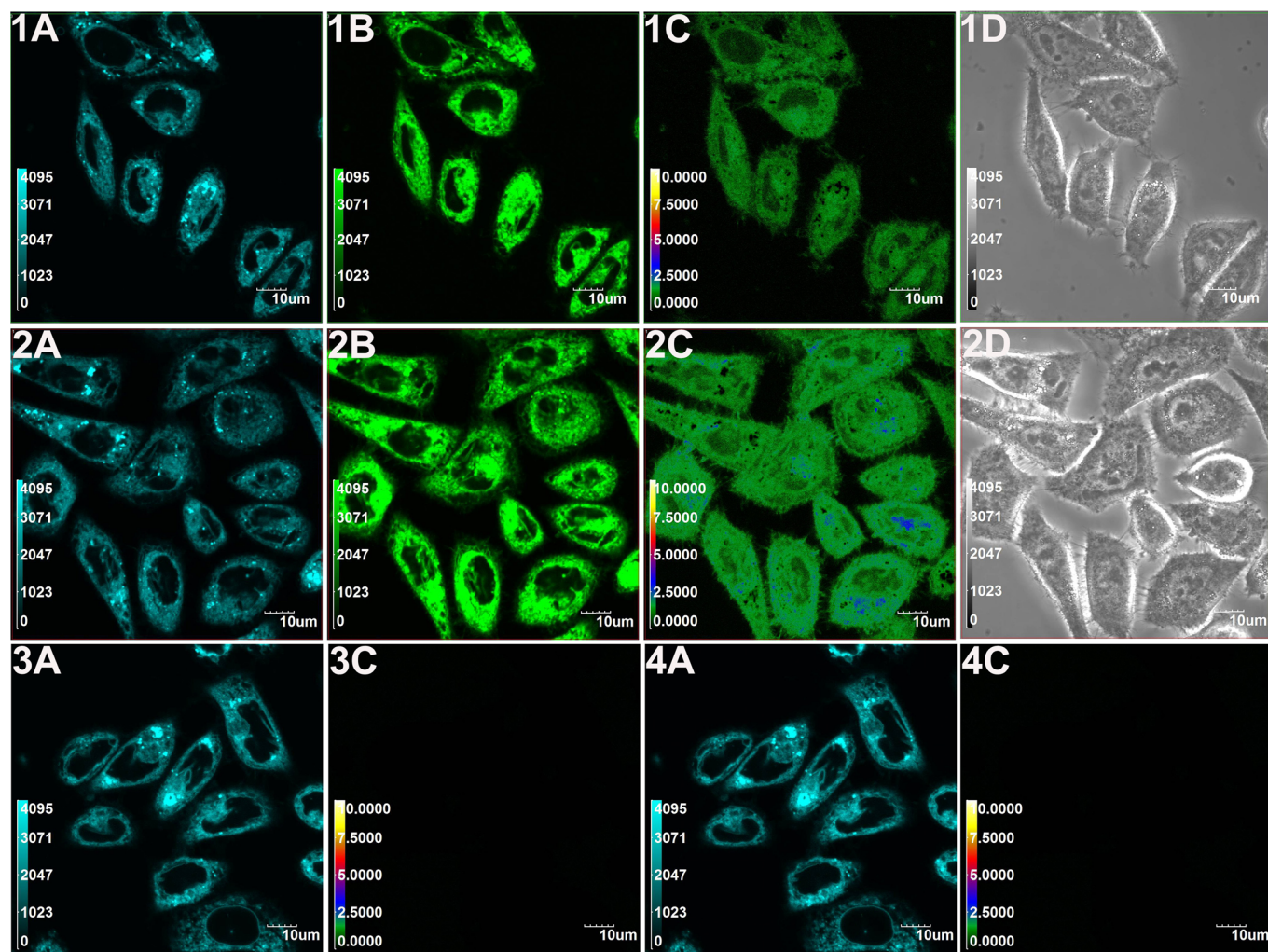


Figure 5 | Confocal fluorescence imaging of endogenous H_2S in living MCF-7 cells using RHP-2. Cells were prestimulated with SNP (200 μM) for 30 min and then incubated with RHP-2 (5 μM) for 40 min (1A, 1B, 1C and 1D). Cells were prestimulated with SNP (400 μM) for 30 min and then incubated with RHP-2 (5 μM) for 40 min (2A, 2B, 2C and 2D). Cells were pretreated with 1 mM PPG for 30 min and then incubated with RHP-2 (5 μM) for 30 min (3A and 3C). Cells in panels 3A and 3C were thereafter treated with SNP (400 μM) for 30 min (4A and 4C). Blue channel images were obtained from 445 nm to 495 nm (1A, 2A, 3A and 4A). Green channel images were obtained from 520 nm to 580 nm (1B and 2B). Ratiometric images ($F_{520-580\text{ nm}}/F_{445-495\text{ nm}}$) were generated by Olympus software (1C, 2C, 3C, and 4C) and the corresponding bright images are shown in 1D and 2D. Scale bars = 10 μm .

reduction in immobility duration in the NaHS group compared to the model group (Supplementary Fig. S18, $p < 0.001$; Fig. S19, $p < 0.001$). Moreover, NaHS administration attenuated CUMS-induced decreases of sulphide concentrations (Fig. 6A, $p < 0.001$, Table S1),

Table 1 | Measurements of sulphide concentrations in the mouse hippocampus

Samples	H_2S^a ($\mu mol\ g^{-1}$ protein)	H_2S^b ($\mu mol\ g^{-1}$ protein)
1	1.78	1.79
2	1.67	1.84
3	1.77	1.78
4	1.60	1.73
5	1.59	1.81
6	1.63	1.88
7	1.59	1.75
8	1.75	1.87
average	1.67 ± 0.08	1.81 ± 0.05

^aMeasurement of sulphide concentrations in the mouse hippocampus using RHP-2.

^bMeasurement of sulphide concentrations in the mouse hippocampus using SFP-2.
Data are presented as the mean \pm SD ($n = 8$)

CBS protein expression (Fig. 6B, $p < 0.001$) and CBS mRNA levels (Fig. 6C, $p < 0.001$) compared to the model group. Consequently, (1) RHP-2 is an effective tool for the determination of different concentrations of endogenous sulphide in the mouse hippocampus; (2) the application of exogenous sulphide has an antidepressant-like effect in mice with CUMS-induced depression; and (3) a significant decrease in sulphide concentrations and the downregulated expression of CBS mRNA and CBS protein were observed in the hippocampus in a mouse model of chronic stress depression, preliminarily suggesting that the reduced production of endogenous H_2S may contribute to the pathogenesis of depression.

Discussion

Tissue sulphide concentrations depend on the homeostasis between enzymatically producing and consuming reactions⁵¹. However, determination conditions and sample pretreatment may have profound effects on sulphide production and consumption in tissues. Traditional detection methods are the methylene blue and ISE methods. These two methods measured biomolecule-bound sulphide rather than free sulphide due to harsh chemical treatment (strong acid or base, respectively) prior to analysis. Sample pretreatment in

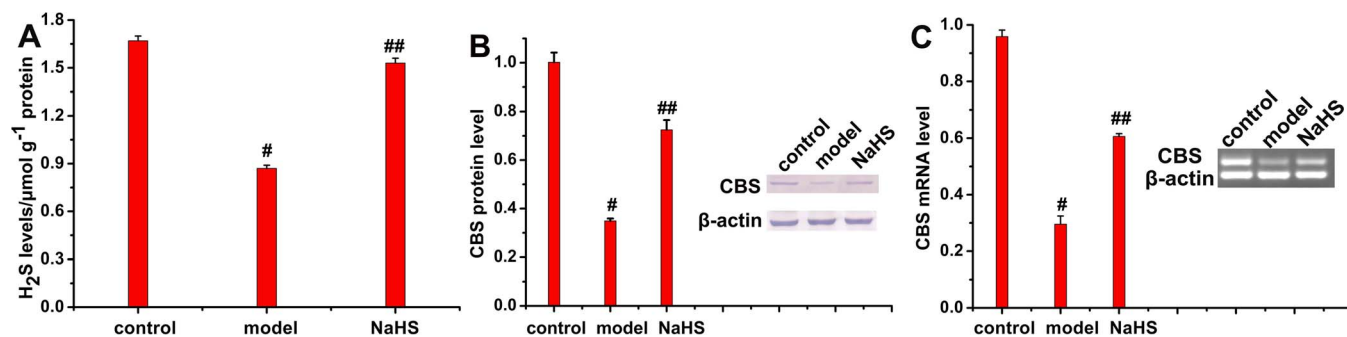


Figure 6 | Reduced sulphide concentrations and CBS expression in the hippocampus in mouse models of CUMS-induced depression. (A) Sulphide concentrations in the mouse hippocampus. Data are presented as the mean \pm SEM ($n = 8$). $^{\#}p < 0.001$ vs. control, $^{##}p < 0.001$ vs. model. (B) CBS protein expression in the mouse hippocampus. Data are presented as the mean \pm SEM ($n = 3$). $^{\#}p < 0.001$ vs. control, $^{##}p < 0.001$ vs. model. (C) CBS mRNA levels in the mouse hippocampus. Data are presented as the mean \pm SEM ($n = 3$). $^{\#}p < 0.001$ vs. control, $^{##}p < 0.001$ vs. model. Full-length blots are presented in Supplementary Figures S20 and S21.

the fluorescent probe-based method does not involve sophisticated sample processing and the addition of chemicals⁴⁸. Specifically, to minimise deviation from the actual value, the following precautions were taken: (1) sample pre-processing was performed in an ice bath to minimise the anabolism and catabolism of sulphide, and the homogenate supernatants were immediately used for the determination; (2) hippocampus tissues were isolated and immediately homogenised within 60 s in PBS buffer (pH 7.4) to trap free hydrogen sulphide as HS⁻; (3) each experiment was conducted at least in triplicate; and (4) we repeated the measurements with our previous probe (SFP-2) to compare with the data using RHP-2.

CUMS is a validated depression model. Throughout the CUMS induction, the animals were subjected to chronic and continuous low stress, and consequently exhibited the apparent behavioural deficits that are signs of human depressive states, such as despair, anhedonia and lack of activation^{52,53}. CUMS induction successfully simulated a depressive-like status in mice by the reduction of sucrose intake and the increase of immobility duration in the forced swimming and tail suspension tests.

CBS, the major H₂S-producing enzyme in the brain, is highly expressed in the hippocampus. Interestingly, we noted that the endogenous H₂S concentrations were markedly reduced in the hippocampus in depressive-like mice after exposure to CUMS. Additionally, CBS mRNA and CBS protein expression were decreased. To the best of our knowledge, we are the first group to obtain preliminary data indicating that decreased levels of endogenous H₂S might be involved in the pathogenesis of depression. Moreover, treatment with NaHS significantly attenuated CUMS-induced decreases of sulphide concentrations and CBS expression, suggesting that the enhanced expression of CBS contributes to the elevation of H₂S concentrations in the mouse hippocampus. Surprisingly, the injection of NaHS resulted in a positive feedback for the enhanced expression of CBS. These results are consistent with several recent publications on the upregulation of CBS/CSE expression by exogenous sulphide. In the studies of Han *et al*, tobacco smoke exposure (TS) reduced the protein expression of CSE and CBS as well as the capacity for H₂S synthesis in mouse lungs, and treatment with NaHS attenuated TS-induced downregulation of CSE and CBS expression⁵⁴. Park observed that unilateral ureteral obstruction (UO) induced a reduction of H₂S levels in the kidney together with decreases in CBS and CSE expression, and NaHS treatment mitigated the decreased kidney H₂S levels and enzyme expressions in the mouse models of UO-induced kidney fibrosis⁵⁵. Zhang reported that plasma H₂S levels and CSE expression in nasal mucosa were decreased in sensitised guinea pigs, and NaHS increased the levels of H₂S accompanied by upregulation of CSE expression⁵⁶. However, the mechanism for NaHS-upregulated CBS/CSE expression is not yet

clear. With the updated information of catabolic fate of H₂S, some studies showed that exogenous sulphide was rapidly consumed by plasma or tissues, and mammals have relatively high capacity to metabolize exogenous administered sulphide^{16,18}. We speculated that the rapid metabolism of exogenous sulphide probably gave a negative feedback for the expression of CBS, thereby elevating expression of CBS. Further studies are necessary to confirm this speculation. Furthermore, our studies demonstrated the antidepressant effects of H₂S. The present findings imply that H₂S might be a potential therapeutic target for chronic stress depression, and the application of exogenous H₂S and H₂S donors may be of therapeutic value in the treatment of depression.

To conclude, we synthesised and applied the ratiometric fluorescent probe RHP-2 for H₂S detection. Probe RHP-2 underwent a blue-to-green fluorescent emission colour change in response to sulphide. Advantages of this H₂S-specific probe include a low detection limit, high sensitivity and selectivity, good photostability and low cytotoxicity. The emission intensity ratios had a good linear relationship with sulphide concentrations in PBS buffer and bovine serum. This probe enabled the ratiometric fluorescence imaging of endogenous H₂S in living cells and the determination of sulphide in the mouse hippocampus. The results using RHP-2 suggest that decreased concentrations of endogenous H₂S may be involved in the pathogenesis of CUMS-induced depression.

Methods

Synthesis of RHP-2. A solution of NAP-NH₂ (27 mg, 0.1 mmol) and 4-dimethylaminopyridine (DMAP) (37 mg, 0.3 mmol) in toluene (8 mL) was cooled to 0°C, which was followed by the dropwise addition of a solution of triphosgene (45 mg, 0.15 mmol) in toluene. The reaction mixture was heated under reflux for 6 h. When cooled to room temperature, the mixture was diluted with dehydrated CH₂Cl₂ (8 mL), followed by the addition of 4-nitrobenzyl alcohol (20 mg, 0.13 mmol). The resulting solution was stirred overnight at room temperature. The reaction was quenched with water (5 mL) and extracted with EtOAc (3 \times 10 mL). The combined organic layers were rinsed with water and saturated brine and dehydrated with Na₂SO₄. The solvent was evaporated, and the crude product was purified by column chromatography on SiO₂ to give the purified product, a white powder. Yield: 16 mg, 35.8%. TLC (silica, hexane: EtOAc, 2:1 v/v): R_f = 0.4; ¹H NMR (400 MHz, DMSO-*d*₆): δ 10.48 (s, 1 H, ArH), 8.70 (d, $J = 8.8$ Hz, 1 H, ArH), 8.49 (d, $J = 7.6$ Hz, 1 H, ArH), 8.46 (d, $J = 8.4$ Hz, 1 H, ArH), 8.28 (d, $J = 8.4$ Hz, 2 H, ArH), 8.18 (d, $J = 8.0$ Hz, 1 H, ArH), 7.83 (t, $J = 8.0$ Hz, 1 H, ArH), 7.76 (d, $J = 8.8$ Hz, 2 H, ArH), 5.42 (s, 2 H, ArCH₂-), 4.01 (t, $J = 7.6$ and 7.2 Hz, 2 H, NCH₂-), 1.56–1.63 (m, 2 H, NCH₂CH₂-), 1.29–1.38 (m, 2 H, -CH₂CH₃), 0.91 (t, $J = 7.2$ Hz, 3 H, -CH₃); ¹³C NMR (100 MHz, DMSO-*d*₆): δ 163.9, 163.3, 154.2, 147.6, 144.6, 140.9, 132.1, 131.4, 129.7, 129.0, 128.7, 126.9, 124.3, 124.1, 122.7, 118.8, 117.7, 65.7, 39.3, 30.1, 20.2, 14.2; HRMS (m/z): [M-H]⁺ calcd. for C₂₄H₂₀N₃O₆, 446.1352; observed, 446.1359.

Fluorometric analyses. All fluorescence measurements were conducted at room temperature on a Hitachi F4600 Fluorescence Spectrophotometer. The RHP-2 probe (CH₃CN) was added to a quartz cuvette. With the probe diluted to 5 μ M with 20 mM PBS buffer, Na₂S was added (Na₂S \cdot 9H₂O serving as the H₂S source in all experiments). The resulting solution was incubated for 40 min. The fluorescence



intensity was measured ($\lambda_{\text{ex}} = 415 \text{ nm}$) with the slit widths of excitation and emission set at 5 nm. The emission spectra ranged from 430 to 650 nm at a velocity of 240 nm/min. The photomultiplier voltage was set at 550 V. Data are presented as the mean \pm SD ($n = 3$).

Cell cultures and fluorescence confocal imaging. The MCF-7 cells were cultured in DMEM media with 10% (v/v) FBS (foetal bovine serum) and penicillin/streptomycin (100 $\mu\text{g}/\text{mL}$) at 37°C in a 5% CO₂ incubator. Cells were permitted to grow to 80% confluence before harvesting and transferring to a coverglass (Lab-Tek® II Chambered Coverglass, NalcoNunc, Naperville, USA). The RHP-2 solution (1.0 mM stock solution in CH₃CN, final concentration 5 μM) was added to the cell media and incubated for 30 min with or without PPG (DL-propargylglycine, 50 mg/L stock solution in DI H₂O)/ZnCl₂ (10 mM stock solution in DI H₂O, final concentration 1 mM) pretreatment. Afterwards, the cells were thrice rinsed with PBS solution (pH = 7.4) to remove excess RHP-2, which was followed by the addition of Na₂S (20 mM stock solution in DI H₂O, final concentration 300 μM) or SNP (sodium nitroprusside, 20 mM stock solution in DI H₂O, final concentration 200 or 400 μM) in PBS for incubation at room temperature. The cells were thrice rinsed with PBS buffer prior to imaging. Confocal fluorescence imaging was performed on an Olympus FV1000 confocal laser scanning microscope with $\times 10$ dry and $\times 60$ oil objectives. The excitation wavelength was 425 nm. The blue fluorescent images were obtained from 445 to 495 nm, and the green fluorescent images were obtained from 520 to 580 nm. The images were obtained at 1024 \times 1024 pixels. Images and data were analysed with Olympus software (FV10-ASW). All data are expressed as the mean \pm SD ($n = 3$).

Determination of sulphide in the mouse hippocampus. For the measurement of sulphide, the mice were sacrificed, and the hippocampus was immediately isolated and homogenised with 9 volumes (w/v) of ice-cold 100 mM PBS buffer (pH 7.4); the homogenate was centrifuged at 10,000 \times g for 10 min at 4°C. All of the procedures were performed in an ice bath, and the homogenate supernatants were immediately transferred for sulphide determination. All fluorescence measurements were recorded on a Hitachi F4600 Fluorescence Spectrophotometer. Protein concentrations of the mouse hippocampus were determined with a Pierce BCA Protein Assay Kit. The determination of sulphide concentration in hippocampus homogenates spiked with Na₂S were used as an internal standard (X, X + 0.4, X + 0.8, X + 1.2 and X + 1.6 μM). Twenty microlitres of 10% homogenate supernatant (final concentration 2%, w/v) was added into Eppendorf tubes containing 69 μL of PBS buffer (100 mM, pH 7.4) and DI H₂O (10, 9.6, 9.2, 8.8 and 8.4 μL , respectively). Thereafter, 0, 0.4, 0.8, 1.2, 1.6 μL of Na₂S stock solution (100 μM) were spiked into the samples as an internal standard, followed by the addition of 1 μL of 1.0 mM RHP-2 probe (final concentration 10 μM). Emission spectra ($\lambda_{\text{ex}} = 415 \text{ nm}$) were determined at the end of a 40-min incubation of the mixture at 37°C. The zero point was obtained by the addition of 1 μL of 100 mM (final concentration 1 mM) ZnCl₂ to trap H₂S in the samples. The sulphide concentration in each sample was calculated using a calibration curve of Na₂S, and the results were expressed as $\mu\text{mol g}^{-1}$ protein. All data are expressed as the mean \pm SD ($n = 3$).

Animals and administration. Adult male Kunming mice weighing 20–25 g were provided by the Experimental Animal Centre of Xuzhou Medical College. All of the experiments were performed in compliance with the Chinese legislation on the use and care of laboratory animals and were approved by the Institutional Animal Care and Use of Xuzhou Medical College. The animals were housed in a room with regulated temperature ($22 \pm 2^\circ\text{C}$) and humidity ($50 \pm 10\%$) on a 12 h light/dark cycle; the animals had *ad libitum* access to standard commercial animal feed and pure water. Mice were acclimatised for 1 week prior to the experiment. Twenty-four mice were randomised into three groups ($n = 8$ each): the control group, without treatment; the model group, 5 consecutive weeks of CUMS induction; and the NaHS group, 5 consecutive weeks of CUMS induction, intraperitoneal injection of NaHS at a daily dose of 5 mg/kg 30 min prior to stress exposure beginning in the 4th week of the experiment. Following the behavioural experiment, mice were sacrificed, and the hippocampus was immediately isolated for experiments or storage at -70°C for subsequent measurements.

Western blot. For western blot analysis, the hippocampus was homogenised in 1/3 (w/v) ice-cold extraction buffer (20 mM Tris-HCl buffer, pH 7.6, 150 mM NaCl, 2 mM EDTA·2Na, 50 mM sodium fluoride, 1 mM sodium vanadate, 1% Nonidet P-40, 1% sodium deoxycholate, 0.1% SDS, 1 mg/ml aprotinin, and 1 mg/ml leupeptin). The homogenates were sonicated 4 times for 30 s at a 20-s interval on a VWR Bronson Scientific sonicator, which was followed by centrifugation at 10,000 \times g for 10 min at 4°C, and the supernatant was collected. Protein concentrations were determined using BCA protein assay kits. Equal amounts of protein (20 μg) were separated by 10% SDS-polyacrylamide gel electrophoresis and transferred to a nitrocellulose membrane (Amersham Pharmacia Biotech). The membrane was blocked with 5% skim milk powder in a washing buffer (Tris-buffered saline containing 0.05% (v/v) Tween 20) for 2 h at 25°C and subsequently incubated overnight with the primary antibodies specific for CBS (1:1000) and β -actin (1:1000). Each membrane was thrice rinsed for 15 min and incubated with either alkaline phosphatase-conjugated secondary antibodies (1:1000, Goat anti-Rabbit IgG antibody) or alkaline phosphatase-conjugated secondary antibodies (1:1000, Horse anti-Mouse IgG antibody), which was followed by visualization by

BCIP/NBT alkaline phosphatase colour development kits. Protein bands were quantified by densitometric analysis using ImageJ analysis software.

Reverse transcriptase-PCR (RT-PCR). For mRNA quantification, total RNA was extracted with the TRI reagent (Sigma-Aldrich, St. Louis, MO, USA). Complementary DNA was synthesised using the High Capacity RNA-to-cDNA kit (*ibid.*) according to the manufacturer's protocol. The housekeeping gene β -actin was used as an internal control for the normalisation of each gene examined. Amplified products were separated by electrophoresis on a 1.25% agarose gel followed by visualisation under a UV transilluminator and photography. To verify reproducibility, each sample was analysed in duplicates in three independent experiments for each gene. The values obtained for the target gene expression were normalised to β -actin and quantified relative to the expression in the control samples. The products were analysed by densitometry using ImageJ analysis software, and quantities of each product were calculated relative to β -actin. The primer sequences specific for CBS were 5' CTGGACATGCACTCAGAAAAG 3' (forward) and 5' TGATAGTCTCCAGGCTTCAA 3' (reverse), and those for β -actin were 5' ATGGTCACGACGATTCCC 3' (forward) and 5' GAGACCTTCAACACC-CCAGC 3' (reverse).

Statistical analyses. All statistical analyses were performed using SPSS software, version 16.0 (SPSS Inc., Chicago, IL, USA). Values are expressed as the mean \pm SD (standard deviation of the mean). The data were analysed with one-way analysis of variance (ANOVA). Statistical significance was set at $p < 0.05$.

- Predmore, B. L., Lefer, D. J. & Gojow, G. Hydrogen sulfide in biochemistry and medicine. *Antioxid. Redox. Signal.* **17**, 119–140 (2012).
- Kabil, O. & Banerjee, R. Redox biochemistry of hydrogen sulfide. *J. Biol. Chem.* **285**, 21903–21907 (2010).
- Stein, A. & Bailey, S. M. Redox Biology of Hydrogen Sulfide: Implications for Physiology, Pathophysiology and Pharmacology. *Redox. Biol.* **1**, 32–39 (2013).
- Hu, L. F., Lu, M., Hon Wong, P. T. & Bian, J. S. Hydrogen sulfide: neurophysiology and neuropathology. *Antioxid. Redox. Signal.* **15**, 405–419 (2011).
- Lefer, D. J. A new gaseous signaling molecule emerges: cardioprotective role of hydrogen sulfide. *Proc. Natl. Acad. Sci. U. S. A.* **104**, 17907–17908 (2007).
- Yang, G., Wu, L. & Wang, R. Pro-apoptotic effect of endogenous H₂S on human aorta smooth muscle cells. *FASEB. J.* **20**, 553–555 (2006).
- Zanardo, R. C. *et al.* Hydrogen sulfide is an endogenous modulator of leukocyte-mediated inflammation. *FASEB. J.* **20**, 2118–2120 (2006).
- Elrod, J. W. *et al.* Hydrogen sulfide attenuates myocardial ischemia-reperfusion injury by preservation of mitochondrial function. *Proc. Natl. Acad. Sci. U. S. A.* **104**, 15560–15565 (2007).
- Kaneko, Y., Kimura, Y., Kimura, H. & Niki, I. L-cysteine inhibits insulin release from the pancreatic beta-cell: possible involvement of metabolic production of hydrogen sulfide, a novel gasotransmitter. *Diabetes.* **55**, 1391–1397 (2006).
- Olson, K. R. The therapeutic potential of hydrogen sulfide: separating hype from hope. *Am. J. Physiol. Regul. Integr. Comp. Physiol.* **301**, R297–312 (2011).
- Ichinohe, A. *et al.* Cystathionine beta-synthase is enriched in the brains of Down's patients. *Biochem. Biophys. Res. Commun.* **338**, 1547–1550 (2005).
- Eto, K. *et al.* Brain hydrogen sulfide is severely decreased in Alzheimer's disease. *Biochem. Biophys. Res. Commun.* **293**, 1485–1488 (2002).
- Hu, L. F. *et al.* Neuroprotective effects of hydrogen sulfide on Parkinson's disease rat models. *Aging. Cell.* **9**, 135–146 (2010).
- Han, Y. *et al.* Modulating effect of hydrogen sulfide on gamma-aminobutyric acid B receptor in recurrent febrile seizures in rats. *Neurosci. Res.* **53**, 216–219 (2005).
- Nagy, P. *et al.* Chemical aspects of hydrogen sulfide measurements in physiological samples. *Biochim. Biophys. Acta.* **1840**, 876–891 (2014).
- Olson, K. R. Is hydrogen sulfide a circulating "gasotransmitter" in vertebrate blood? *Biochim. Biophys. Acta.* **1787**, 856–863 (2009).
- Small, J. M. & Hintelmann, H. Methylene blue derivatization then LC-MS analysis for measurement of trace levels of sulfide in aquatic samples. *Anal. Bioanal. Chem.* **387**, 2881–2886 (2007).
- Whitfield, N. L. *et al.* Reappraisal of H₂S/sulfide concentration in vertebrate blood and its potential significance in ischemic preconditioning and vascular signaling. *Am. J. Physiol. Regul. Integr. Comp. Physiol.* **294**, R1930–1937 (2008).
- Shen, X., Peter, E. A., Bir, S., Wang, R. & Kevil, C. G. Analytical measurement of discrete hydrogen sulfide pools in biological specimens. *Free Radic. Biol. Med.* **52**, 2276–2283 (2012).
- Hughes, M. N., Centelles, M. N. & Moore, K. P. Making and working with hydrogen sulfide: The chemistry and generation of hydrogen sulfide in vitro and its measurement in vivo: a review. *Free Radic. Biol. Med.* **47**, 1346–1353 (2009).
- Peng, H. *et al.* Thiol reactive probes and chemosensors. *Sensors* **2**, 15907–15946 (2012).
- Peng, H., Chen, W., Burroughs, S. & Wang, B. Recent advances in fluorescent probes for the detection of hydrogen sulfide. *Curr. Org. Chem.* **17**, 641–653 (2013).
- Lippert, A. R., New, E. J. & Chang, C. J. Reaction-based fluorescent probes for selective imaging of hydrogen sulfide in living cells. *J. Am. Chem. Soc.* **133**, 10078–10080 (2011).
- Peng, H. *et al.* A fluorescent probe for fast and quantitative detection of hydrogen sulfide in blood. *Angew. Chem. Int. Ed. Engl.* **50**, 9672–9675 (2011).



25. Liu, C. *et al.* Capture and visualization of hydrogen sulfide by a fluorescent probe. *Angew. Chem. Int. Ed. Engl.* **50**, 10327–10329 (2011).
26. Sun, W. *et al.* A two-photon fluorescent probe with near-infrared emission for hydrogen sulfide imaging in biosystems. *Chem. Commun.* **49**, 3890–3892 (2013).
27. Cao, X., Lin, W., Zheng, K. & He, L. A near-infrared fluorescent turn-on probe for fluorescence imaging of hydrogen sulfide in living cells based on thiolysis of dinitrophenyl ether. *Chem. Commun.* **48**, 10529–10531 (2012).
28. Chen, Y. *et al.* A ratiometric fluorescent probe for rapid detection of hydrogen sulfide in mitochondria. *Angew. Chem. Int. Ed. Engl.* **52**, 1688–1691 (2013).
29. Wang, X. *et al.* A Near-infrared ratiometric fluorescent probe for rapid and highly sensitive imaging of endogenous hydrogen sulfide in living cells. *Chem. Sci.* **2013**, DOI: 10.1039/c3sc50369k
30. Liu, T., Xu, Z., Spring, D. R. & Cui, J. A lysosome-targetable fluorescent probe for imaging hydrogen sulfide in living cells. *Org. Lett.* **15**, 2310–2313 (2013).
31. Sasakura, K. *et al.* Development of a highly selective fluorescence probe for hydrogen sulfide. *J. Am. Chem. Soc.* **133**, 18003–18005 (2011).
32. Ueno, T. & Nagano, T. Fluorescent probes for sensing and imaging. *Nat. Methods.* **8**, 642–645 (2011).
33. Zhu, W., Dai, M., Xu, Y. & Qian, X. Novel nitroheterocyclic hypoxic markers for solid tumor: synthesis and biological evaluation. *Bioorg. Med. Chem.* **16**, 3255–3260 (2008).
34. Dai, M. *et al.* Versatile nitro-fluorophore as highly effective sensor for hypoxic tumor cells: design, imaging and evaluation. *J. Fluoresc.* **18**, 591–597 (2008).
35. Tanabe, K., Hirata, N., Harada, H., Hiraoka, M. & Nishimoto, S. Emission under hypoxia: one-electron reduction and fluorescence characteristics of an indolequinone-coumarin conjugate. *Chem. Biochem.* **9**, 426–432 (2008).
36. Kiyose, K. *et al.* Hypoxia-sensitive fluorescent probes for in vivo real-time fluorescence imaging of acute ischemia. *J. Am. Chem. Soc.* **132**, 15846–15848 (2010).
37. Xu, K. *et al.* High selectivity imaging of nitroreductase using a near-infrared fluorescence probe in hypoxic tumor. *Chem. Commun.* **49**, 2554–2556 (2013).
38. Cui, L. *et al.* A new prodrug-derived ratiometric fluorescent probe for hypoxia: high selectivity of nitroreductase and imaging in tumor cell. *Org. Lett.* **13**, 928–931 (2011).
39. Montoya, L. A. & Pluth, M. D. Selective turn-on fluorescent probes for imaging hydrogen sulfide in living cells. *Chem. Commun.* **48**, 4767–4769 (2012).
40. Wu, M. Y., Li, K., Hou, J. T., Huang, Z. & Yu, X. Q. A selective colorimetric and ratiometric fluorescent probe for hydrogen sulfide. *Org. Biomol. Chem.* **10**, 8342–8347 (2010).
41. Reja, S. I., Kumar, N., Sachdeva, R., Bhalla, V. & Kumar, M. d-PET coupled ESIPT phenomenon for fluorescent turn-on detection of hydrogen sulfide. *RSC. Advances.* **3**, 17770–17774 (2013).
42. Wang, R. *et al.* A highly selective turn-on near-infrared fluorescent probe for hydrogen sulfide detection and imaging in living cells. *Chem. Commun.* **48**, 11757–11759 (2012).
43. Zhao, W., Zhang, J., Lu, Y. & Wang, R. The vasorelaxant effect of H₂S as a novel endogenous gaseous K(ATP) channel opener. *EMBO. J.* **20**, 6008–6016 (2001).
44. Doeller, J. E. *et al.* Polarographic measurement of hydrogen sulfide production and consumption by mammalian tissues. *Anal. Biochem.* **341**, 40–51 (2005).
45. Furne, J., Saeed, A. & Levitt, M. D. Whole tissue hydrogen sulfide concentrations are orders of magnitude lower than presently accepted values. *Am. J. Physiol. Regul. Integr. Comp. Physiol.* **295**, R1479–1485 (2008).
46. Wintner, E. A. *et al.* A monobromobimane-based assay to measure the pharmacokinetic profile of reactive sulphide species in blood. *Br. J. Pharmacol.* **160**, 941–957 (2010).
47. Ishigami, M. *et al.* A source of hydrogen sulfide and mechanism of its release in the brain. *Antioxid. Redox. Signal.* **11**, 205–214 (2009).
48. Qian, Y. *et al.* A Fluorescent Probe for rapid detection of hydrogen sulfide in blood plasma and brain tissues in mice. *Chem. Sci.* **3**, 2920–2923 (2012).
49. Qian, Y. *et al.* Selective fluorescent probes for live-cell monitoring of sulphide. *Nat. Commun.* **2**, 495 (2011).
50. Chen, W. L. *et al.* Antidepressant-like and anxiolytic-like effects of hydrogen sulfide in behavioral models of depression and anxiety. *Behav. Pharmacol.* **2013**, DOI: 10.1097/FBP.0b013e3283654258.
51. Vitvitsky, V., Kabil, O. & Banerjee, R. High turnover rates for hydrogen sulfide allow for rapid regulation of its tissue concentrations. *Antioxid. Redox. Signal.* **17**, 22–31 (2012).
52. Katz, R. J. Animal model of depression: pharmacological sensitivity of a hedonic deficit. *Pharmacol. Biochem. Behav.* **16**, 965–968 (1982).
53. Willner, P., Towell, A., Sampson, D., Sophokleous, S. & Muscat, R. Reduction of sucrose preference by chronic unpredictable mild stress, and its restoration by a tricyclic antidepressant. *Psychopharmacology.* **93**, 358–364 (1987).
54. Han, W., Dong, Z., Dimitropoulou, C. & Su, Y. Hydrogen sulfide ameliorates tobacco smoke-induced oxidative stress and emphysema in mice. *Antioxid. Redox. Signal.* **15**, 2121–2134 (2011).
55. Jung, K. J. *et al.* Involvement of hydrogen sulfide and homocysteine transsulfuration pathway in the progression of kidney fibrosis after ureteral obstruction. *Biochim. Biophys. Acta.* **1832**, 1989–1997 (2013).
56. Shaoqing, Y. *et al.* Down-regulation of endogenous hydrogen sulphide pathway in nasal mucosa of allergic rhinitis in guinea pigs. *Allergol. Immunopathol.* **37**, 180–187 (2009).

Acknowledgments

This project was financed by grants from the National Natural Science Foundation of China (81341084 to Y.L.) and the Jiangsu Natural Science Foundation (BK20111547 to J.Z.). The project was also funded by the Priority Academic Programme Development of Jiangsu Higher Education Institutions, the Zhen Xing Project of XZMC, the Laboratory of Encephalopathy and Bioinformation of Jiangsu Province (Jsb1204 to L.Z.), the Natural Science Foundation for Colleges and Universities in Jiangsu Province (14KJB350005 to L.Z.) the Postdoctoral Science Foundation of China (2012M521125 to Y.L.), and the Graduate Student Innovation Plan of Jiangsu Province (CXZZ13_0996). We thank Professor H.Y. Dong (Research Center for Neurobiology) for help with cell-based imaging experiments.

Author contributions

J.Z. and Y.L. conceived the idea and directed the work. J.Z. and L.Z. designed the experiments. L.Z., W.M. and L.L. performed the synthesis. L.Z. and F.Z. performed the cell-based imaging. L.Z. and W.M. performed the in vitro fluorescence tests and quantitative tests in the mouse hippocampus. W.M. and C.L. performed the animal studies. Y.X. provided the molecular calculation data. All authors contributed to the data analysis and to writing the manuscript.

Additional information

Supplementary information accompanies this paper at <http://www.nature.com/scientificreports>

Competing financial interests: The authors declare no competing financial interests.

How to cite this article: Zhang, L. *et al.* Selective detection of endogenous H₂S in living cells and the mouse hippocampus using a ratiometric fluorescent probe. *Sci. Rep.* **4**, 5870; DOI:10.1038/srep05870 (2014).



This work is licensed under a Creative Commons Attribution-NonCommercial-NoDerivs 4.0 International License. The images or other third party material in this article are included in the article's Creative Commons license, unless indicated otherwise in the credit line; if the material is not included under the Creative Commons license, users will need to obtain permission from the license holder in order to reproduce the material. To view a copy of this license, visit <http://creativecommons.org/licenses/by-nc-nd/4.0/>